ECOLOGY LETTERS cnrs WILEY

Altered precipitation dynamics lead to a shift in herbivore dynamical regime

Adam Pepi[1,2] | Marcel Holyoak[3] | Richard Karban[2]

[1]Graduate Group in Ecology, University of California Davis, Davis, CA, USA

[2]Department of Entomology and Nematology, University of California Davis, Davis, CA, USA

[3]Department of Environmental Science and Policy, University of California Davis, Davis, CA, USA

Correspondence
Adam Pepi, Graduate Group in Ecology, University of California Davis, Davis, CA 95616, USA.
Email: adampepi@gmail.com

Funding information
National Science Foundation, Grant/Award Number: NSF-LTREB-1456225

Editor: Dave Hodgson

Abstract

The interaction between endogenous dynamics and exogenous environmental variation is central to population dynamics. Although investigations into the effects of changing mean climate are widespread, changing patterns of variation in environmental forcing also affect dynamics in complex ways. Using wavelet and time series analyses, we identify a regime shift in the dynamics of a moth species in California from shorter to longer period oscillations over a 34-year census, and contemporaneous changes in regional precipitation dynamics. Simulations support the hypothesis that shifting precipitation dynamics drove changes in moth dynamics, possibly due to stochastic resonance with delayed density-dependence. The observed shift in climate dynamics and the interaction with endogenous dynamics mean that predicting future population dynamics will require information on both climatic shifts and their interaction with endogenous density-dependence, a combination that is rarely available. Consequently, models based on historical data may be unable to predict future population dynamics.

KEYWORDS
climate change, delayed density-dependence, population dynamics, stochastic resonance

INTRODUCTION

The dynamics of populations reflect the interplay between endogenous demographic and exogenous environmental drivers. Since its inception, population ecology has focused on debates about the relative contribution of these components to the generation of several salient phenomena observed in the dynamics of natural and laboratory populations, particularly cyclic fluctuations (Andrewartha & Birch, 1954; Barraquand et al., 2017; Nicholson, 1933). More recently, it has been recognised that both endogenous and exogenous drivers play important roles in generating observed population dynamics, and that endogenous deterministic dynamics and exogenous environmental noise or perturbations may combine to generate differing dynamics than would be expected for either component alone (Barraquand et al., 2017; Bjørnstad & Grenfell, 2001; Turchin, 2003). There has been additional motivation to understand the effects of climate on population dynamics as the effects of global climate change on the planet's biota have become more apparent (Parmesan, 2006; Walther et al., 2002). Climate change is expected to result in increased climate variability (Coumou & Rahmstorf, 2012), as well as alterations to patterns of large-scale climate oscillations (Simon Wang et al., 2017), both of which are important drivers of local population dynamics. In a prominent example, changes in oceanic temperature oscillation regimes have resulted in dramatic changes to precipitation patterns in California (Simon Wang et al., 2017), with large impacts to society and natural ecosystems.

Climate variation can have direct effects on interannual fluctuations in population size or may interact in complex ways with endogenous dynamics of populations.

For example, environmental perturbations can sustain population oscillations that might otherwise decay to a stable equilibrium (Barraquand et al., 2017; Tomé & De Oliveira, 2009). Climate change has also appeared to cause the collapse of population cycles of many species across Europe (Cornulier et al., 2013; Ims et al., 2008). Environmental perturbations with different spectra of variability can also amplify, dampen or impose their own spectra on oscillatory populations depending on the "colour" (temporal autocorrelation) of environmental spectra relative to the spectra of the endogenous dynamics of the population (Greenman & Benton, 2003). Changing climate can also interact in a non-stationary way with population dynamics, such as transient effects of long-term climate oscillations on epidemic disease cycles (Cazelles et al., 2005; Rodó et al., 2002). However, testing for such effects on population dynamics of other kinds of organisms requires rarely available long-term population data.

In this study, we examined how changing precipitation dynamics interact with the endogenous population dynamics of an extensively studied insect species, the Ranchman's tiger moth (*Arctia virginalis*). We analysed 34 years of census data from northern California, over a period during which there have been significant shifts in the dynamics of regional climate (Simon Wang et al., 2017). Using time series analyses and simulations, we tested for changes in population dynamics, and compared multiple possible mechanisms for observed shifts. Using simulations, we tested the hypotheses that shifting dynamics were because 1. underlying dynamics were first masked and later amplified by precipitation, 2. underlying dynamics were first amplified and later masked by precipitation or 3. dynamical shifts were driven completely exogenously by changing precipitation dynamics.

MATERIALS AND METHODS

Description of system

Ranchman's tiger moth (*Arctia virginalis*) is a univoltine, day-active Arctiine moth, native to much of the western United States. Adult moths emerge in late spring or early summer and have a flight period of several weeks during which they do not feed. Eggs are laid on low vegetation or litter in early summer; small caterpillars hatch soon after eggs are laid. Early instar caterpillars are heavily preyed upon by ground nesting ants, and are potentially food limited during seasonal senescence of vegetation in Mediterranean summers (Karban et al., 2013, 2017). Time series analyses have shown that greater precipitation during the previous year results in greater population growth, possibly due to increased food availability during the summer drought (Karban & de Valpine, 2010; Karban et al., 2017). Caterpillars feed continuously over the winter period and do not diapause in California.

After this, they move up to feed on higher vegetation and become more visible in late winter in California. Caterpillars are generalists, with a preference for alkaloid-containing hosts (English-Loeb et al., 1993; Karban et al., 2010). Caterpillars are also frequently attacked by tachinid parasitoids, *Thelaira americana* (Karban & de Valpine, 2010), which are specialists on Arctiine moths (Arnaud, 1978), and may functionally be specialists on Ranchman's tiger moth at our study site, the Bodega Marine Reserve. However, analyses have suggested that parasitism has little effect on caterpillar population dynamics (Karban & de Valpine, 2010). Caterpillar populations at the Bodega Marine Reserve and other sites often exhibit high mortality rates after high population density years due to a granulovirus. Monitoring at Bodega and other sites has shown delayed density-dependent infection and mortality rates due to granulovirus (Pepi et al. 2021).

Censuses

Caterpillar censuses were conducted on perennial evergreen yellow bush lupine (*Lupinus arboreus*) bushes at Bodega Marine Reserve in Sonoma County, California (38°19'05"N, 123°04'12"W). The number of caterpillars on 10 lupine bushes in the same patch was counted yearly from 1986 to 2019 (>10 in 1986). Bushes were censused in the last week of March each year. Previous repeated censuses within a year between late February and the end of March suggest that population estimates were unlikely to vary significantly due to changes in seasonal phenology from year to year (Karban and Grof-Tisza, unpublished data), because of the long development period of caterpillars and their limited mobility during this stage. The same lupine bushes were censused each year; however, the identity of bushes changed because these lupines were short lived (<7 year). To account for variation in sampling effort, area of each lupine bush censused was measured to calculate caterpillar density per m^2 (plotted as caterpillars per 100 m^2 in Figure 1 for legibility). Precipitation was recorded at the site as part of ongoing climate monitoring by the University of California and using a rain gauge at the study site (US Weather Bureau type manual rain gauge prior to 1992 and an optical rain gauge ORG-815, Optical Scientific, Gaithersburg, MD since 1992 with a Hydrological Services TB4 tipping bucket, Campbell Scientific, Ogden, UT since 2003). For analyses, total annual precipitation within the hydrologic year was calculated (from October 1st of the previous year to September 30th of the current year).

Statistical analyses

To test for non-stationary relationships between precipitation and caterpillar dynamics over time, wavelet analysis
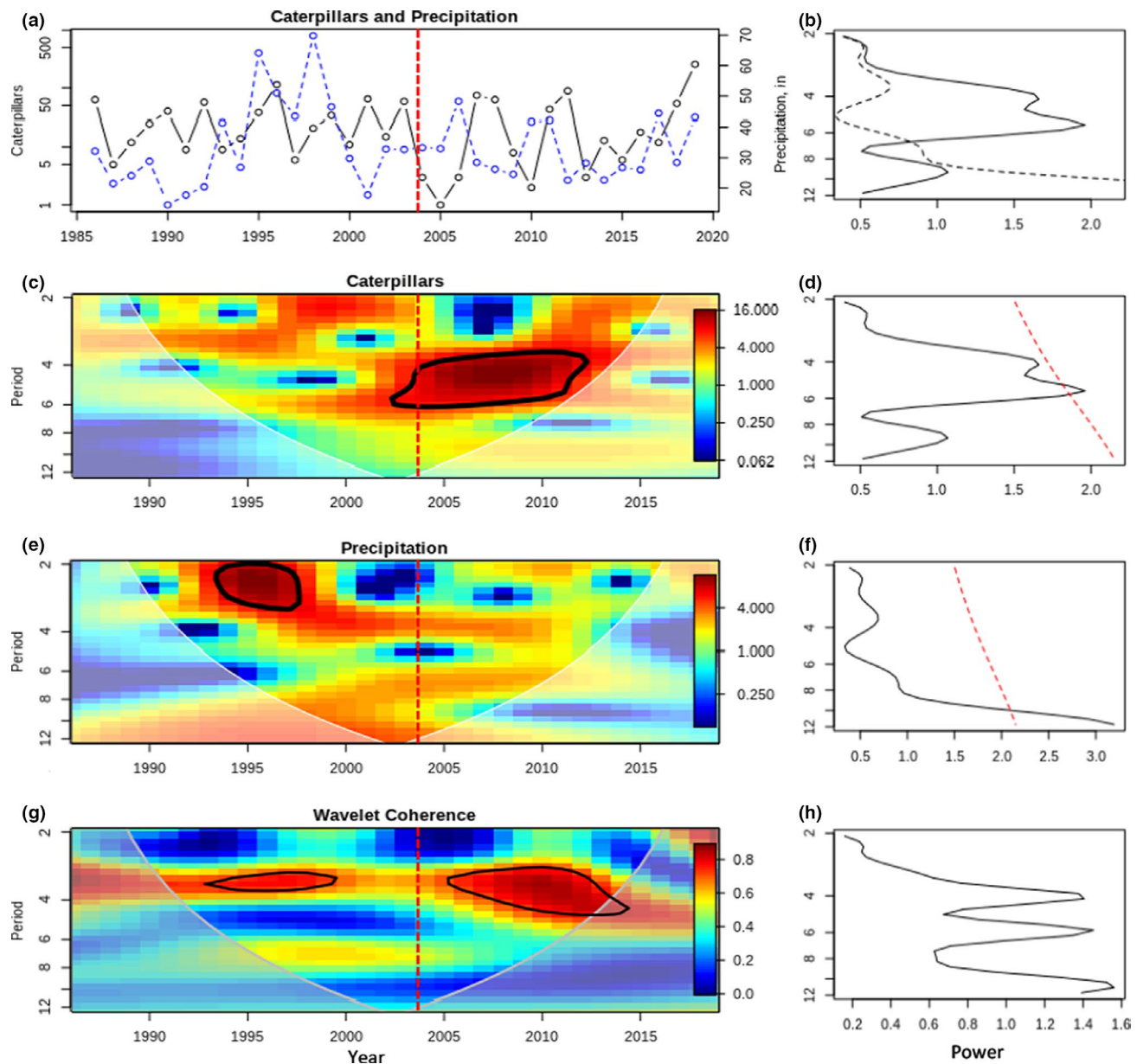
FIGURE 1 (a) Time series of caterpillar population counts per 100 m² (solid black line) and total annual precipitation (dashed blue line); (c) local wavelet transform of caterpillar population counts; (e) local wavelet transform of total annual precipitation; (g) wavelet coherence between total annual precipitation and caterpillar population counts; (b, d and f) global spectra of (a, c and e); (h) global coherence of (g), total annual precipitation and caterpillar population counts. The dashed red line through (a, c, e and g) represents the time threshold found in the change-point analysis including precipitation. Caterpillar density and spectral period are shown on a log scale; total annual precipitation is shown on the right axis. Solid black lines in (c, e and g) delimit regions of significant periodicity or coherence at a 95% confidence level from a bootstrap test. Colour bars in (c, e and g) show the scale power from low (blue) to high (red). Caterpillar wavelet spectrum is shown in (a) with a solid line, and precipitation wavelet spectrum is shown with a dashed line. Dashed red lines in (d and f) show the 95% confidence threshold from a bootstrap test; peaks to the right of the line represent significant periodicity

was conducted separately on logged and scaled caterpillar and scaled precipitation time series, and as wavelet coherence analyses on both series (Figure 1). Scaling was accomplished by subtracting the mean and dividing by the standard deviation (scale() in R). Analyses were conducted using the package BIWAVELET (Gouhier et al., 2019), using Morlet wavelet transforms. In addition, change-point analyses were conducted using the SEGLM and TSDYN packages (Antonio et al., 2009;

Stigler, 2019), with a model containing direct and delayed density-dependence, and a separate model also including precipitation as a covariate. We included precipitation as a covariate based on previous knowledge that precipitation was important to dynamics. We included direct density-dependence based on previous detection in time series analyses (Karban & de Valpine, 2010), and delayed density-dependence based on wavelet periodogram results and the observation of delayed density-dependent

mortality from granulovirus in field studies (Pepi et al., 2021). Models with and without a threshold (C) were compared using AIC. Break point models were of the form:

$$X_t \sim Normal(a_{0,1} + a_{1,1}X_{t-1} + a_{2,1}X_{t-2} + \beta_{1,1}Precip_{t-1}, \sigma_1^2) \mid t \leq C$$

$$X_t \sim Normal(a_{0,2} + a_{1,2}X_{t-1} + a_{2,2}X_{t-2} + \beta_{1,2}Precip_{t-1}, \sigma_2^2) \mid t \geq C,$$

in which X_t is log population density [$ln(count/area)$], a_0 is the intercept, a_1 is direct density-dependence, a_2 is delayed density-dependence and β_1 is the effect of precipitation, σ^2 is the variance, with a separate parameter estimate for each before and after the threshold.

Bayesian state-space population models using a Poisson observation process were constructed to test for direct and delayed density-dependence and effects of precipitation. We conducted this as a separate step from testing for thresholds to avoid identifiability issues due to limited data availability. We primarily examined a model with the same process structure as breakpoint models, including direct and delayed density-dependence and an effect of precipitation, based on *a priori* knowledge about the system. For comparison, models with all possible combinations of variables were generated and compared using WAIC (Vehtari et al., 2017). State-space models were fit to the time series from 1986 to 2004 and 2004 to 2019 separately and results compared, based on findings of change-point analyses. The full state-space model was of the form:

$$Y_t \sim Poisson\left(\exp\left(X_t\right) * area_t\right)$$

$$X_t \sim Normal\left(a_0 + a_1X_{t-1} + a_2X_{t-2} + \beta_1Precip_{t-1}, \sigma^2\right),$$

in which Y_t is caterpillar count, X_t is the estimated population density state on a log scale, $area_t$ is the area of lupine sampled, a_0 is the intercept, a_1 is direct density-dependence, a_2 is delayed density-dependence, β_1 is the effect of precipitation and σ^2 is the process variance. Models were fitted in JAGS with interface in R using RJAGS (Plummer, 2019) and R2JAGS (Yu-Sung Su & Yajima 2015). We used a vague regularising Gaussian prior for all parameters [$Normal(0, 10)$], except for the process variance (σ^2), for which we used a uniform prior [$Uniform(0, 10)$]. Model convergence was assessed using the CODA (Martyn et al. 2019) package, by visualising chains (Figures S1–3) and the $\hat{R}$ convergence criterion (Gelman & Rubin, 1992). We also conducted one-step ahead simulations as posterior predictive checks (Figures S4–6), for which p-values were 0.5 ± 0.03, indicating acceptable model fit. Models were fitted using three MCMC chains of 20,000 iterations, with 1000 iterations of burn-in. All $\hat{R}$ values were <1.001.

To ascertain the mechanisms driving shifts in dynamics, we conducted deterministic simulations by projecting populations into the future using parameter values sampled from the posteriors of fitted state-space process models. Simulations were also conducted with fitted density-dependence parameters, but with all precipitation effects drawn from the posterior of the model with the highest estimated effect of precipitation (from the second half of the series; $\beta_1 = 0.922$). Another simulation was conducted using the fitted process model from the second part of the series, but with density-dependent parameters (a_1, a_2) set to zero. For simulations, observed starting population sizes were used, and observed precipitation values were used for the entire period. For each mechanistic scenario, 10,000 simulations were conducted, each based on a separate draw from posteriors. Simulated population trajectories were wavelet transformed, and a dissimilarity relative to the true population series was calculated based on the method of Rouyer *et al.* (2008b) (Table S3, Figures S7–8), all using BIWAVELET (Gouhier et al., 2019).

RESULTS

Caterpillar population dynamics exhibited a clear regime shift during our study. Wavelet spectrograms show that dominant oscillatory periods of caterpillar and precipitation dynamics shifted from short-period (2–3 years) to long-period oscillations (4–6 years; Figure 1c and e), although periodicity was only significant at the 95% level for precipitation in the first part of the series (2- to 3-year periodicity from ~1992 to 1999) and caterpillars in the second part of the series (4- to 6-year periodicity from ~2003 to 2013). Precipitation dynamics changed after ca. 1999, and caterpillar dynamics changed shortly thereafter (ca. 2002). Wavelet coherence between precipitation and caterpillar numbers shifted from a 3-year period in the early part of the series to a 3- to 6-year period after ca. 2005 (Figure 1g), suggesting a role of precipitation in shifts in caterpillar population dynamics. The observed shift in precipitation dynamics, in turn, was likely caused by shifting oceanic climate oscillations; the Pacific Decadal Oscillation and offshore sea surface temperature switched from a warm to a cold phase after 1999, which resulted in shifts in dynamics of several marine species at that time (Cloern et al., 2010; Thomson et al., 2010). A similar climate regime of high-amplitude, long-period oscillations between multi-year drought and high precipitation is expected to be the norm for California in the future (Swain et al., 2018).

Change-point analyses found a change in dynamics with a threshold in 2002 (ΔAIC = 1.2 relative to model without a threshold) in a model without precipitation, or in 2004 in a model including precipitation (ΔAIC = 6.5 relative to model without a threshold). Before the threshold, direct density-dependence was estimated to be negative and this became positive after the threshold, although there was limited evidence that these estimates were different from zero ($0.10 > p > 0.09$; see Table 1). In models that included precipitation, its effects were always near zero before the threshold, and strongly positive after the threshold (Table 1). Delayed density-dependence had

negative parameter estimates in all models, with the most evidence for delayed density-dependence after the threshold in the model without precipitation ($p = 0.019$), and weaker evidence otherwise ($p > 0.2$).

Results from Bayesian Poisson state-space models corresponded broadly with those from the change-point analyses, showing a shift in dynamics from the first to the second period. The full model was an acceptable fit relative to other model structures tested, though large differences were not detected due to the state-space structure and limited data availability (Table S1; ΔWAIC < 2 for all models). Ninety-percent high-density posterior intervals (HDPI) that are superior for characterising MCMC posteriors (because of more samples in the tails; Kruschke, 2014) show the following: Considering the full model fitted to the entire series (1986–2019), direct density-dependence was weak ($a_1 = -0.11$; 90% HDPI: -0.23 to 0.47), delayed density-dependence was negative ($a_2 = -0.3$; 90% HDPI: -0.63 to 0.03]) and there was a weak positive effect of rainfall ($\beta_1 = 0.30$; 90% HDPI: -0.08 to 0.70; Figure 2). For the first part of the series (1986–2004), direct density-dependence was negative ($a_1 = -0.63$; 90% HDPI: -1.19 to -0.10), delayed density-dependence was negative but weak ($a_2 = -0.27$; 90% HDPI: -0.78 to 0.26) and the effect of precipitation was weak ($\beta_1 = 0.26$; 90% HDPI: -0.17 to 0.68; Figure 2). For the second part of the series (2004–2019), direct density-dependence was positive ($a_1 = 0.46$; 90% HDPI: 0.03 to 0.82), delayed density-dependence was negative but weak ($a_2 = -0.19$; 90% HDPI: -0.63 to 0.36) and the effect of precipitation was stronger and positive ($\beta_1 = 0.92$; 90% HDPI: 0.2 to 1.75; Figure 2). Overall, the results of these models provide evidence for a shift from negative to positive direct density-dependence from the first to the second part of the series, with non-overlapping 90% intervals between the two parts ($a_1 = -1.19$ to -0.13 vs. 0.03 to 0.82), although 95% intervals did have a marginal overlap ($a_1 = -1.29$ to 0.03 vs. -0.05 to 0.96; Figure 2). This corresponds with a shift from Type-III to Type-IV dynamics (Figure 3) and a shift from shorter to longer period dynamics.

The results from simulation analyses suggested that the long-period dynamics observed in the second part of the series (2004–2019) could best recreate the observed dynamics. Specifically, there was some evidence that endogenous dynamics as parameterised from the second part of the series best recovered the observed shift in

dynamical regime when used to simulate dynamics for the entire series, based on the maximum *a posteriori* dissimilarity calculated from wavelet transforms (Figure 4, S1, Table S3; Rouyer et al., 2008; Gouhier et al., 2019). This was the case both in simulations which used the original fitted precipitation parameters, and in simulations in which the effect of precipitation was set to the same value to examine solely the effect of different endogenous dynamics (lowest dissimilarity: $d = 17.6$; whole series: $d = 22.1$, 18.5; first part: $d = 22.8$, 21.4; Figure 4, S1, Table S3). Simulations including density-dependence reproduced dynamics somewhat better ($d = 17.6$) than simulations without density-dependence ($d = 19.7$). The broad posterior intervals of simulation results indicated substantial uncertainty as to the mechanisms driving observed shifts (Figure 4). However, to the extent that we are interested in the question of whether specific endogenous dynamics (i.e. specific parameter values) underlie the observed shift in dynamics, the point estimates from the second part of the series best reproduced dynamics. Overall, results were consistent with the interpretation that the shift in dynamics was driven either by an interaction between endogenous dynamics and precipitation, or possibly solely by precipitation (Figure 4).

DISCUSSION

Our analyses together suggest that over the census period, the changing structure of variation in precipitation dynamics interacted with the structure of endogenous dynamics of caterpillar populations to generate novel dynamics. This resulted in higher amplitude, long-period oscillations in the second part of the series (2004–2019), in which both the lowest (2005) and the highest (2019) caterpillar population densities were observed. This is in contrast with the first part of the census (1986–2004) which was characterised by weak lower amplitude and short-period oscillations. These shifts in oscillatory period corresponded with a shift from negative direct and delayed density-dependence (Type-III dynamics) to positive direct and negative delayed density-dependence (Type-IV dynamics). Although many parameter posterior intervals overlapped zero, there was strong statistical evidence for our main hypothesis, showing a shift from negative to positive direct density-dependence during the

TABLE 1 Results of change-point analysis, including parameter estimates and P values, from models with and without precipitation, before and after change-point thresholds

| Model	Period	$a_{1[P]}$	$a_{2[P]}$	$\beta_{1[P]}$
Without Precipitation	1986–2002	-0.56 [$p = 0.098$]	-0.44 [$p = 0.211$]	
	2002–2019	0.35 [$p = 0.109$]	-0.52 [$p = 0.019$]	
With Precipitation	1986–2004	-0.57 [$p = 0.091$]	-0.41 [$p = 0.209$]	-0.01 [$p = 0.098$]
	2004–2019	0.510 [$p = 0.027$]	-0.286 [$p = 0.218$]	1.27 [$p = 0.026$]
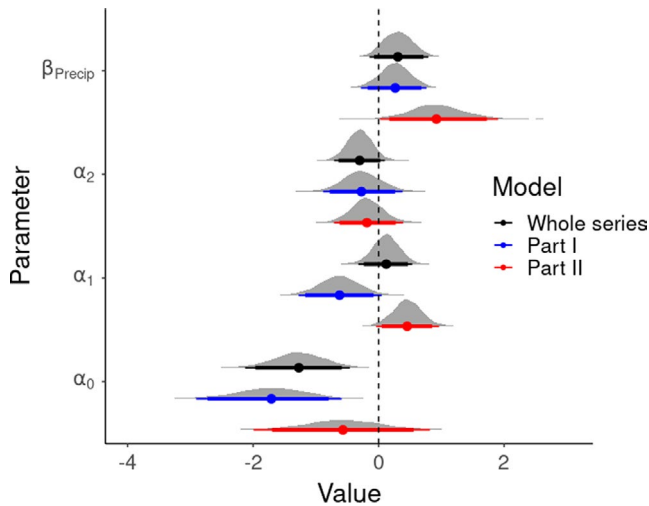
FIGURE 2 Bayesian posterior 90% and 95% (broad to narrow lines) posterior intervals, and point estimates of parameters from Poisson state-space models. Estimates from the whole series are shown in black (1986–2019), before the threshold in blue (1986–2004) and after the threshold in red (2004–2019)
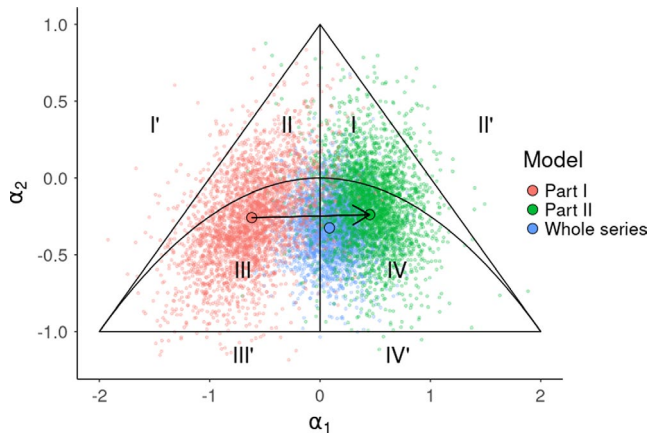
FIGURE 3 Posterior distributions of Bayesian state-space models fit to the first part of the series (1986–2004), the second part of the series (2004–2019) and the whole series (1986–2019), plotted in the Royama parameter plane, showing a shift from Type-III to Type-IV dynamics. Open circles represent the median of the posterior distributions

study (Figures 2 and 3). This shift in dynamics appears to have been due to changing patterns of variation in environmental forcing and illustrates the complexity of forecasting impacts of changes in both mean and pattern of variation in future climates on population dynamics.

Simulation studies have shown that environmental noise can resonate with the dominant period of the deterministic endogenous dynamics of a system if the noise spectra include the period of the deterministic system (Alonso et al., 2007; Royama, 1992). Environmental variation may also impose its own spectral signature on population dynamics with different dominant periods (Greenman & Benton, 2003). Given these observations, there are multiple possible mechanistic explanations for the shift in dynamics observed in this study. One
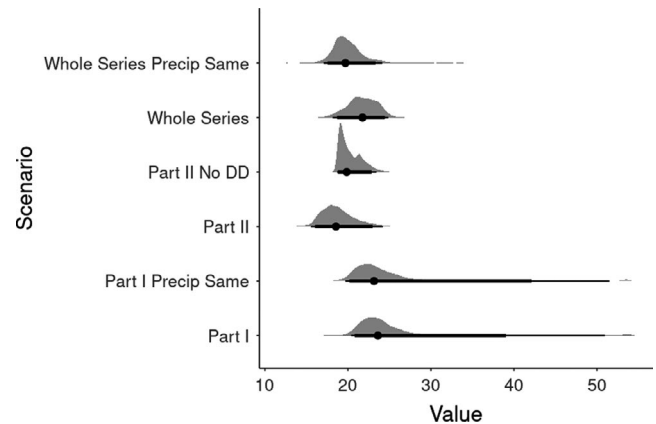
FIGURE 4 Simulation 90% and 95% (broad to narrow lines) posterior intervals and point estimates of dissimilarity values relative to the true population trajectories, from multiple mechanistic scenarios

possible interpretation is that the interaction between the endogenous dynamical structure of this population with changing exogenous perturbation (i.e. precipitation) obscured the endogenous dynamics in one part of the series, but not the other (Ranta et al., 2000). Another interpretation is that dynamical shifts may have been entirely externally forced by changing precipitation dynamics. We distinguished between these possibilities by simulating deterministic population trajectories from fitted state-space models using observed precipitation, which indicated that the dynamics from the second part of the series were somewhat more likely to have represented the underlying endogenous dynamics of the system. This indicates that short-period oscillations in precipitation may have interfered with delayed density-dependence in the endogenous dynamics to generate the observed population dynamics in the first half of the caterpillar time series. By imposing short-period oscillations onto population dynamics, external forcing by precipitation may have created only the appearance of negative direct density-dependence. During the second half of the series, longer period oscillations of precipitation may have resonated with delayed density-dependence and generated high-amplitude long-period oscillations. This interpretation is supported by the fact that simulations including negative direct density-dependence (i.e. the model from the first part of the series) prevented the resonance of precipitation with delayed density-dependence and did not recreate the original dynamics quite as effectively as models with positive direct density-dependence (Figure 4, S7–8, Table S3). Furthermore, the possibility that observed shifts in dynamics were driven completely externally by precipitation seems less likely because simulations lacking density-dependence did not as effectively recover the original shift in dynamics as simulations including density-dependence. However, if we consider the uncertainty of parameter estimates in the simulation

results, we cannot be confident in distinguishing between alternative scenarios, as all simulation posteriors overlap substantially (Figure 4). Nonetheless, despite the limited information contained within our 34-year population time series, our simulations allowed us to compare the relative evidence for alternate mechanisms that might have caused the observed shift.

The dynamics that we describe during the first part of the series are consistent with previous work, which indicated that precipitation positively affects caterpillar population growth rates and interacts with endogenous dynamics of overcompensating negative direct density-dependence (Karban & de Valpine, 2010; Karban et al., 2017). Mechanisms proposed to explain the effect of precipitation include limited resources during summer drought (Karban & de Valpine, 2010), or negative effects of precipitation on predatory ants (Karban et al., 2017). Parasitism and viral infection are potential mechanisms for both direct and delayed density-dependence in this population, as they are in many insects and particularly Lepidoptera (Myers & Cory, 2013, 2016). Parasitism and viral infection can induce density-dependence in insect population dynamics when parasitoids are host specific and display numerical responses to host density and when virus transmission depends on host density (Myers & Cory, 2013). Delays in the action of density-dependence may be caused by delayed numerical responses of parasitoids (Myers & Cory, 2013), or a greater prevalence of covert viral infections or viral occlusion bodies in the environment after high-density years (Myers & Cory, 2016). Long-term monitoring data revealed no delayed density-dependent parasitism in this population (Karban & de Valpine, 2010). However, laboratory rearing of *A. virginalis* from multiple monitored populations suggested a delayed-density-dependent rate of viral infection (Pepi et al. 2021) as is the case in many Lepidoptera (Anderson & May, 1980; Myers & Cory, 2013, 2016).

In contrast, the dynamics of the second part of the series (2004–2019) were not predictable from our previous understanding of caterpillar population dynamics derived from analyses of time series that were long by ecological standards (20 years, 1986–2006; Karban & de Valpine, 2010). This type of non-stationarity due to shifts in climatic regimes has large implications for forecasting and managing populations of threatened or pest species, because such shifts have the potential to obfuscate predictions about management actions. Ecological forecasting has become an urgent goal in light of global change and unprecedented human pressures on the biosphere (Clark et al., 2001). Whereas most literature has focused on predicting ecological state variables (e.g. population size; Dietze, 2017), we examined how changing patterns of climate interacted with endogenous population drivers to qualitatively change dynamics. This illustrates the importance of considering the interaction between endogenous population drivers and exogenous climate variation in projecting population dynamics into the future, and argues that incorporating changes in patterns of climate into predictions is essential.

The fact that the qualitative range of dynamics in populations is to some extent limited (i.e. there are not 10 million types of population dynamics; Lawton, 1992) makes predicting shifts in population dynamics due to climate change a more attainable prospect. Consistent with this, most populations have either first or second order, and either chaotic or non-chaotic dynamics (Types I–IV and I'–IV' in Figure 2; also see Royama, 1992), in addition to some other important axes of variation (Barraquand et al., 2017; Turchin, 2003). Ecologically, the presence of overcompensating (Types II–III) density-dependence, a stable equilibrium (Type I) or longer period cycles (Type IV) have important effects on species interactions, ecosystem dynamics, and how climate is likely to affect dynamics (Ims et al., 2008; Ranta et al., 2000). Mechanistic studies separating endogenous from exogenous components of dynamics can distinguish whether observed dynamics, such as cycles, arise from different mechanisms. Some of these mechanisms include self-sustaining or noise-sustained second-order dynamics, externally forced first-order dynamics (Barraquand et al., 2017) and non-cyclic dynamics that mask endogenous second-order dynamics, as we found support for in the present study (Greenman & Benton, 2003). The application of methods such as those implemented in the present study can help distinguish between different possible combinations of endogenous and exogenous components of a system that might have generated the observed dynamics. Doing so will improve our ability to understand how changes in exogenous forcing due to climate change are likely to affect future population dynamics.

AUTHORSHIP

AP, RK and MH conceived the study, AP conducted the analyses and wrote the manuscript, RK collected the census data and RK and MH provided editorial advice.

PEER REVIEW

The peer review history for this article is available at https://publons.com/publon/10.1111/ele.13756.

DATA AVAILABILITY STATEMENT

The supporting data and code are archived on Zenodo at https://doi.org/10.5281/zenodo.4633950.

ORCID

Adam Pepi https://orcid.org/0000-0002-8253-6938
Marcel Holyoak https://orcid.org/0000-0001-9727-3627

REFERENCES

Alonso, D., McKane, A.J. & Pascual, M. (2007) Stochastic amplification in epidemics. *Journal of the Royal Society, Interface*, 4, 575–582.

Anderson, R.M. & May, R.M. (1980) Infectious diseases and population cycles of forest insects. *Science*, 210, 658–661.

Andrewartha, H.G. & Birch, L.C. (1954) *The distribution and abundance of animals*. Chigago: University of Chicago Press.

Antonio, F., Aznarte, J. & Stigler, M. (2009) tsDyn: Time series analysis based on dynamical systems theory.

Arnaud, P.H. (1978) Host Parasite Catalog of North American Tachinidae (Diptera). Department of Agriculture, Science and Education Administration.

Barraquand, F., Louca, S., Abbott, K.C., Cobbold, C.A., Cordoleani, F., DeAngelis, D.L. et al. (2017) Moving forward in circles: challenges and opportunities in modelling population cycles. *Ecology Letters*, 20, 1074–1092.

Bjørnstad, O.N. & Grenfell, B.T. (2001) Noisy clockwork: time series analysis of population fluctuations in animals. *Science*, 293, 638–643.

Cazelles, B., Chavez, M., McMichael, A.J. & Hales, S. (2005) Nonstationary influence of El Niño on the synchronous dengue epidemics in Thailand. *PLoS Medicine*, 2, 313–318.

Clark, J.S., Carpenter, S.R., Barber, M., Collins, S., Dobson, A., Foley, J.A. et al. (2001) Ecological forecasts: An emerging imperative. *Science*, 293, 657–660.

Cloern, J.E., Hieb, K.A., Jacobson, T., Sansó, B., Di Lorenzo, E., Stacey, M.T. et al. (2010) Biological communities in San Francisco Bay track large-scale climate forcing over the North Pacific. *Geophysical Research Letters*, 37, 1–6.

Cornulier, T., Yoccoz, N.G., Bretagnolle, V., Brommer, J.E., Butet, A., Ecke, F. et al. (2013) Europe-wide dampening of population cycles in keystone herbivores. *Science*, 340, 63–66.

Coumou, D. & Rahmstorf, S. (2012) A decade of weather extremes. *Nature Climate Change*, 2, 491–496.

Dietze, M.C. (2017) Prediction in ecology: A first-principles framework. *Ecological Applications*, 27, 2048–2060.

English-Loeb, G.M., Brody, A.K. & Karban, R. (1993) Host-plant-mediated interactions between a generalist folivore and its tachinid parasitoid. *Journal of Animal Ecology*, 62, 465.

Gelman, A. & Rubin, D.B. (1992) Inference from iterative simulation using multiple sequences. *Statistical Science*, 7, 457–472.

Gouhier, T.C., Grinsted, A. & Simko, V. (2019) R package biwavelet: Conduct univariate and bivariate wavelet analyses.

Greenman, J.V. & Benton, T.G. (2003) The amplification of environmental noise in population models: Causes and consequences. *American Naturalist*, 161, 225–239.

Ims, R.A., Henden, J.A. & Killengreen, S.T. (2008) Collapsing population cycles. *Trends in Ecology & Evolution*, 23, 79–86.

Karban, R. & de Valpine, P. (2010) Population dynamics of an Arctiid caterpillar-tachinid parasitoid system using state-space models. *Journal of Animal Ecology*, 79, 650–661.

Karban, R., Grof-Tisza, P. & Holyoak, M. (2017) Wet years have more caterpillars: Interacting roles of plant litter and predation by ants. *Ecology*, 98(9), 2370–2378.

Karban, R., Karban, C., Huntzinger, M., Pearse, I. & Crutsinger, G. (2010) Diet mixing enhances the performance of a generalist caterpillar, Platyprepia virginalis. *Ecological Entomology*, 35, 92–99.

Karban, R., Mata, T.M., Grof-Tisza, P., Crutsinger, G. & Holyoak, M.A. (2013) Non-trophic effects of litter reduce ant predation and determine caterpillar survival and distribution. *Oikos*, 122, 1362–1370.

Kruschke, J. (2014) Doing Bayesian data analysis: A tutorial with R, JAGS, and Stan.

Lawton, J.H. (1992) There are not 10 million kinds of population dynamics. *Oikos*, 63, 337–338.

Martyn, A., Best, N., Cowles, K., Vines, K., Bates, D., Almond, R., et al. (2019). Package 'coda': Output Analysis and Diagnostics for MCMC.

Myers, J.H. & Cory, J.S. (2013) Population cycles in forest lepidoptera revisited. *Annual Review of Ecology Evolution and Systematics*, 44, 565–592.

Myers, J.H. & Cory, J.S. (2016) Ecology and evolution of pathogens in natural populations of Lepidoptera. *Evolutionary Applications*, 9, 231–247.

Nicholson, A.J. (1933) The balance of animal populations. *Journal of Animal Ecology*, 2, 132–178.

Parmesan, C. (2006) Ecological and evolutionary responses to recent climate change. *Annual Review of Ecology Evolution and Systematics*, 37, 637–669.

Pepi, A., Pan, V. & Karban, R. (2021). Influence of delayed density and ultraviolet radiation on caterpillar granulovirus infection and mortality. *bioRxiv*, Preprint. 2021.03.22.436482.

Plummer, M. (2019) rjags: Bayesian graphical models using MCMC.

Ranta, E., Lundberg, P., Kaitala, V. & Laakso, J. (2000) Visibility of the environmental noise modulating population dynamics. *Proceedings of the Royal Society B-Biological Sciences*, 267, 1851–1856.

Rodó, X., Pascual, M., Fuchs, G. & Faruque, A.S.G. (2002) ENSO and cholera: A nonstationary link related to climate change? *Proceedings of the National Academy of Sciences*, 99, 12901–12906.

Rouyer, T., Fromentin, J.-M., Stenseth, N.C. & Cazelles, B. (2008) Analysing multiple time series and extending significance testing in wavelet analysis. *Marine Ecology Progress Series*, 359, 11–23.

Royama, T. (1992) *Analytical population dynamics*. London: Chapman & Hall.

Simon Wang, S.Y., Yoon, J.H., Becker, E. & Gillies, R. (2017) California from drought to deluge. *Nature Climate Change*, 7, 465–468.

Stigler, M. (2019). seglm: Segmented/threshold regression methods.

Swain, D.L., Langenbrunner, B., Neelin, J.D. & Hall, A. (2018) Increasing precipitation volatility in twenty-first-century California. *Nature Climate Change*, 8, 427–433.

Thomson, J.R., Kimmerer, W.J., Brown, L.R., Newman, K.B., Nally, R.M., Bennett, W.A. et al. (2010) Bayesian change point analysis of abundance trends for pelagic fishes in the upper San Francisco Estuary. *Ecological Applications*, 20, 1431–1448.

Tomé, T. & De Oliveira, M.J. (2009) Role of noise in population dynamics cycles. *Physical review. E, Statistical, nonlinear, and soft matter physics*, 79, 1–8.

Turchin, P. (2003) *Complex population dynamics: A theoretical/empirical synthesis*. Princeton: Princeton University Press.

Vehtari, A., Gelman, A. & Gabry, J. (2017) Practical Bayesian model evaluation using leave-one-out cross-validation and WAIC. *Statistics and Computing*, 27, 1413–1432.

Walther, G.-R., Post, E., Convey, P., Menzel, A., Parmesan, C., Beebee, T.J.C. et al. (2002) Ecological responses to recent climate change. *Nature*, 416, 389–395.

Yu-Sung, S. & Yajima, M. (2015) R2jags: Using R to run "JAGS."

SUPPORTING INFORMATION

Additional supporting information may be found online in the Supporting Information section.